

REFINED MODELLING AND ANALYSIS OF BUILDING AGGREGATES FOR THE ASSESSMENT OF SEISMIC RESPONSE

*Original*

REFINED MODELLING AND ANALYSIS OF BUILDING AGGREGATES FOR THE ASSESSMENT OF SEISMIC RESPONSE / Villar, Sofia; Di Trapani, Fabio; Di Benedetto, Marilisa; Petracca, Massimo; Camata, Guido. - ELETTRONICO. - (2024), pp. 1-10. (Intervento presentato al convegno 18th World Conference on Earthquake Engineering (WCEE2024) tenutosi a Milano, Italia nel 30th June to 5th July 2024).

*Availability:*

This version is available at: 11583/2998421 since: 2025-03-20T11:01:34Z

*Publisher:*

IAEE - International Association for Earthquake Engineering

*Published*

DOI:

*Terms of use:*

This article is made available under terms and conditions as specified in the corresponding bibliographic description in the repository

*Publisher copyright*

(Article begins on next page)

## REFINED MODELLING AND ANALYSIS OF BUILDING AGGREGATES FOR THE ASSESSMENT OF SEISMIC RESPONSE

S. Villar<sup>1</sup>, F. Di Trapani<sup>1</sup>, M. Di Benedetto<sup>1</sup>, M. Petracca<sup>2</sup>, G. Camata<sup>3</sup>

<sup>1</sup> Dipartimento di Ingegneria Strutturale, Edile e Geotecnica, Politecnico Di Torino, Turin, Italy,  
[fabio.ditrapani@polito.it](mailto:fabio.ditrapani@polito.it)

<sup>2</sup> ASDEA Software, Pescara, Italy

<sup>3</sup> Dipartimento di Ingegneria e Geologia, Università di Chieti-Pescara, Pescara, Italy

**Abstract:** *Unreinforced masonry (URM) buildings constitute a large portion of Italian-built heritage. URM derive from the process of expansion, completion and transformation of the structural units, especially in the historical city centers. Masonry aggregates can be arranged in a large number of possible configurations, which can include different interstorey heights, different number of stories, different planar shapes and different masonry typologies. However, the major uncertainty is related to the degree of connection between the structural units, which significantly conditions the response. Because of these reasons, the assessment of URM aggregate is not simple and deserves in-depth investigation. In this paper, a reference building aggregate is modelled and analyzed under different arrangement conditions. The numerical model makes use of homogenized masonry approach by means of 2D shell-layered elements, which can account both for the in-plane and out-of-plane response. The model is realized with the STKO software platform for OpenSees. Different boundary conditions are analyzed, namely the deformability of floors, and the composition of the aggregate. Nonlinear static and dynamic analyses are carried out for the different case-studies highlighting the influence of the aforementioned conditions on the response of the structural units and on the extent of the so-called "aggregate effect".*

### 1 Introduction

Recent seismic events have brought to light the vulnerability of unreinforced masonry structures. As historical centers expanded, new masonry structures were added to existing ones, creating what we commonly refer to as "Aggregate Buildings." These structures are inherently complex, composed of units with varying materials, construction methods, slab rigidity, and boundary conditions. Understanding their seismic response has posed an ongoing research challenge that has led to a more conservative approach in their seismic assessment, which typically treats the units as isolated structures. However, this approach overlooks the potential beneficial impact of the interaction between these units, known as the "Aggregate Effect."

Various studies have studied this effect by comparing the response of each unit within the aggregate to its behavior as an isolated structure through numerical simulations. The predominant modeling method chosen is the Equivalent Frame Method (EFM), used in (Brunelli, et al., 2022), (Angiolilli, Lagomarsino, Cattari, & Degli Abbati, 2021), (Bernardini, et al., 2019), which proved to be successful in capturing the aggregate effect. Moreover, the influence of slab rigidity on these structures was explicitly examined in a recent paper by

(Angiolilli, et al., 2023), where different aggregate cases were studied under varying degrees of unit-to-unit connection and slab flexibility using non-linear static analyses. However, the studies concluded that the EFM did not account for combined in-plane and out-of-plane mechanisms, which become relevant when flexible diaphragms are present. In contrast, other authors provided numerical investigations on large URM compounds using more detailed finite element modelling approaches such as the use of 2D (Ferrito, et al., 2016) and 3D elements (Valente, et al., 2019), or the discrete element method (Ulrich, et al., 2015).

Within this context, this paper presents a numerical investigation into the seismic behaviour of URM aggregates, using a three-structural unit aggregate as a reference under two slab conditions: rigid and flexible. The structural model is developed in OpenSees (McKenna, et al., 2000) with the assistance of the STKO software platform (Petracca, et al., 2017). A refined homogenized modelling approach is employed for the masonry, utilizing 2D layered-shell finite elements. The assessment of the aggregate effect is conducted through non-linear static and dynamic analyses in the longitudinal direction of the aggregate. From these analyses, the response of individual units is extracted and compared to their respective individual models. Results will show that the aggregate effect provides a beneficial impact on the seismic performance depending on the position of a structural unit within the building aggregate and the flexibility of the slab.

## 2 Numerical model of unreinforced masonry buildings

### 2.1 Finite Element model in STKO

The numerical model of masonry aggregates was carried entirely in STKO, a software platform for OpenSees. Masonry walls behaviour was simulated as a homogenized material using the *ASDCConcrete3D*, a non-linear constitutive model that accounts for different behaviours for both tension and compression states (Petracca, et al., 2023). Additionally, encompasses the *crackPlanes* feature that allows the creation of multiple cracking surfaces and enhances its performance during cyclic and dynamic analyses by activating the anisotropy of internal. As an option, this constitutive model offers the possibility to utilize the implicit/explicit (*IMPL-EX*) integration method to improve analysis convergence and reduce computational effort (Olive, et al., 2008). The material was inserted into a *layeredShell* type of section and combined with the *ASDShellQ4*, a shell element enhanced to prevent geometry distortion, to improve the capturing of combined effect of in-plane and OOP mechanisms while still benefiting from the analysis speed of a 2D shell model (Xie, et al., 2015), (Chen, et al., 2004). Overt the openings present in the model; a brick lintel is introduced as a mean to prevent damaged spandrel elements from falling and causing convergence issues. To avoid overestimation of the spandrel's resistance, the lintel is surrounded by a contact material designed to fail prematurely in tension and consent the sliding of the lintel. The slabs were modelled using 1D elastic beam elements, that are connected to the masonry by a penalty-based embedded condition. For the two different slab typologies considered for the aggregate building, different modelling choices were adopted. The rigid slab was simulated by introducing a rigid diaphragm condition that consented only displacements along the x and y direction, and the rotation about the (vertical) Z -axis. Flexible slabs were modelled by merging an elastic wood plate of 3cm to the beams to provide limited flexibility.

### 2.2 Validation of the homogenized masonry approach

#### *Description of the building, experimental test, and numerical FE model*

To validate the modelling approach and fine-tune the essential parameters governing the constitutive model, a numerical replication of a full-scale test on a masonry building structure was performed. This test had originally been conducted at the University of Pavia, as documented in (Magenes, et al., 1995). The structure consists of four 250mm-thick walls, measuring 6m x 4.4m in plan and 6.4m in height. All walls are rigidly connected except for the "Door Wall," which is linked to the opposite "Window Wall" through spaced 140mm-high steel "I" profiles, creating a flexible diaphragm. Vertical loads were transmitted through concrete block beams, with a load of 248.4 kN on the first floor and 236.8 kN on the second floor, approximately 10 kN/m<sup>2</sup> per floor. The University of Pavia's experimental test employed a quasi-static cyclic assessment, exerting four uniform forces on the building, with two forces applied on each floor, all in the direction parallel to the "Door Wall."

The STKO numerical model, depicted in Figure 1, employed the modelling techniques detailed in section 2.1 with exception of the beam to wall connection. In this case, due to the orientation of the beams and the presence of punctual push forces, a basic embedded condition was not adequate for effective load transfer to

the masonry. This led to localized damage and beam detachment. To resolve this, a rigid region around each beam was created using the *Rigid Link* command. Material properties were derived from material tests conducted at the University of Pavia (Binda, et al., 1994), (Anthoine, et al., 1995), which were in support of experimental tests on a full-scale masonry building structure (Magenes & Calvi, 1994), (Magenes, et al., 1995). These experiments established a masonry compressive strength of 6.2 MPa and an elastic modulus of 1490 MPa. Initial fracture energy values were obtained based on these parameters using FIB Model Code (2010) and were refined during the calibration process. Two different numerical simulations were performed on the model, a monotonic analysis on both “Front Wall” and the “Back Wall”, and a static-cyclic analysis on the “Door Wall”.

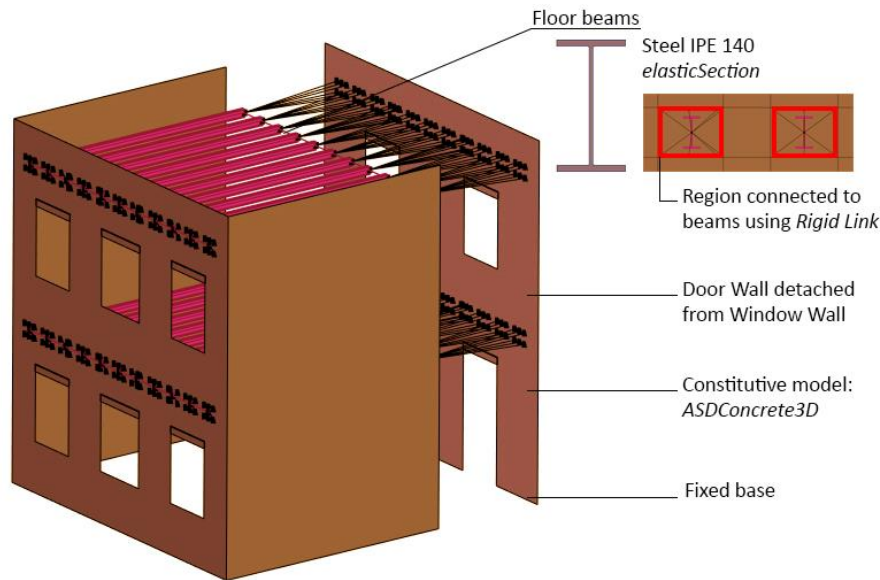


Figure 1. Exploded 3D view of the calibration model.

*Numerical monotonic and cyclic response*

During the monotonic tests, the model underwent two pushover analyses. The first involving the application of a uniform lateral force profile to the "Door Wall" while measuring the displacement at the wall's top and the reaction force at its base. In the second analysis, the focus was on pushing the "Window Wall" instead. These analyses were conducted using displacement control with the incorporation of an Adaptive Time Step to ensure convergence. The findings presented in Figure 2 a, b; reveal a strong alignment between the numerical outcomes and the cyclic test envelope conducted on the building. When comparing the two scenarios, specifically the "Window Wall" case, a distinction becomes evident. In the experimental curve, the peak occurs at 12 mm, and the elastic phase concludes earlier, while in the numerical model, the peak is reached at 5 mm, followed by a rapid reduction in resistance. This variation can be attributed to dissimilar crack propagation behaviours observed in a homogenized model as opposed to a physical masonry sample, especially in cases involving low tensile strength. In the physical sample, cracks tend to follow mortar joints, leading to a gradual decline in resistance. In contrast, the homogenized masonry model illustrates cracks taking the most direct path across the structure, resulting in the numerical model exhibiting higher resistance before experiencing a sudden decline. Moreover, the numerical model was able to reproduce the crack pattern reported in the study (Figure 2 b, c, e, f). The calibrated parameters for the monotonic analysis are presented in Table 1.

Table 1. Calibrated material parameters for monotonic analysis.

| Tensile strength $f_t$ [MPa] | Tensile fracture energy $G_t$ [N/mm] | Compressive strength $f_m$ [MPa] | Compressive fracture energy $G_c$ [N/mm] | Elastic modulus $E_m$ [MPa] |
|------------------------------|--------------------------------------|----------------------------------|--|-----------------------------|
| 0.15                         | 0.07                                 | 6.2                              | 0.14                                     | 1490                        |

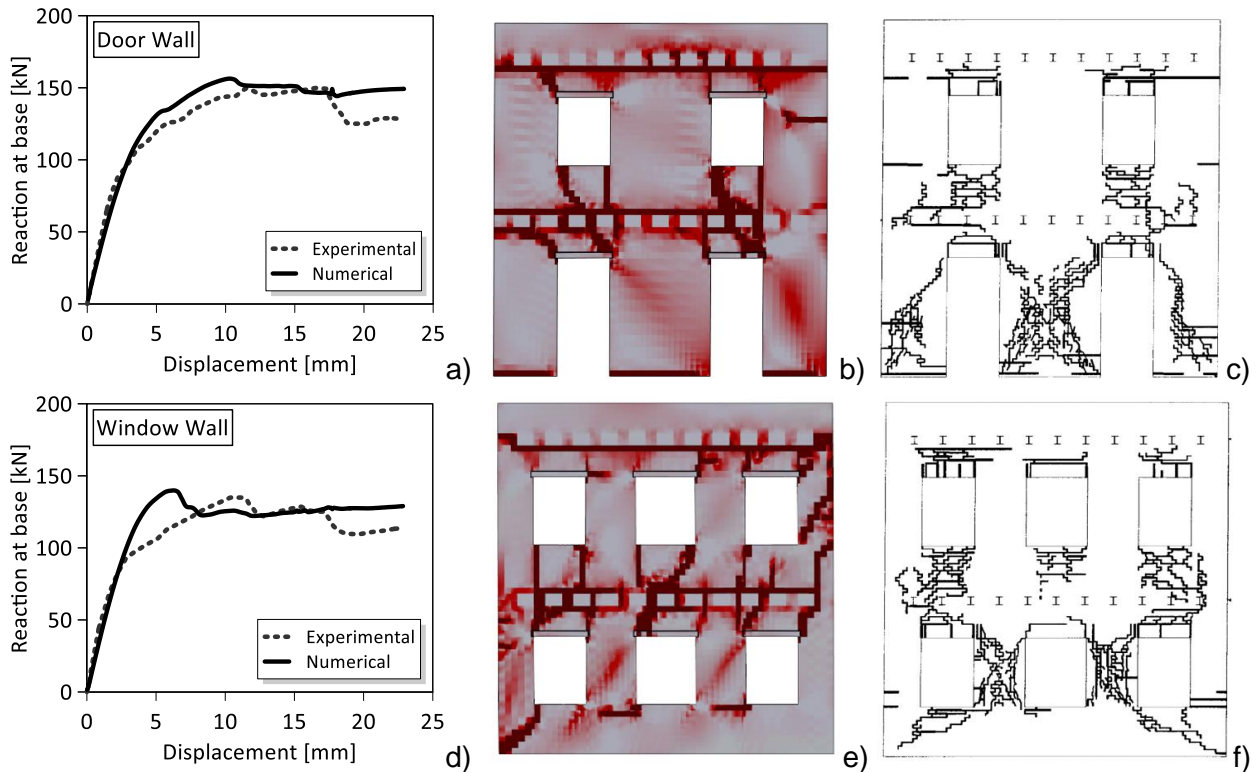


Figure 2. Numerical vs. experimental comparison: a) Pushover curves comparison b) Numerical crack pattern c) Experimental crack pattern.

The cyclic analysis of the numerical model presented additional challenges. Initially, the model used the same material parameters as the monotonic test, revealing a notable strength loss when transitioning from the positive to negative cycle side, despite minimal negative displacement. To address this issue, the *crackPlanes* command was introduced. By activating anisotropy in the internal variables, it was able to create multiple fracture surfaces and restrict the damage to the current principal stress direction, rather than affecting all directions. On a second instance, the shape of the cycles was improved by introducing the plasticity in tension factor, limited to 0.5 with respect to of internal concrete-based plasticity calculated by STKO. Finally, the tensile fracture energy was slightly increased to 0.1 N/mm to obtain a better match of the envelope during softening phase. The analysis maintained the uniform lateral force distribution imposed in the experimental setup. Numerical results (Figure 3) closely aligned with the experimental response in terms of overall shape of the curve and crack pattern. However, a notable stiffness and resistance difference appeared during the initial cycles that can be attributed to the limitations of a concrete-based model to mimic masonry behaviour.

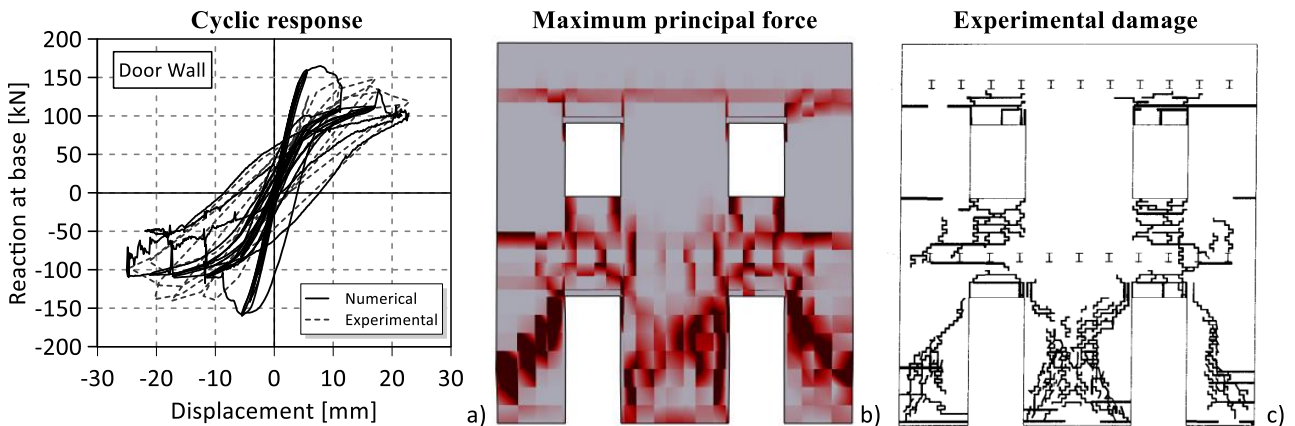


Figure 3. Cyclic analysis of the “Door Wall”: a) cyclic response comparison; b) numerical crack pattern; c) experimental crack pattern

### 2.3 Aggregate reference building: FE model and analysis settings

The reference building aggregate consists of three individual units, each spanning three stories. The central unit (Unit 2) shares a common dividing wall with the external units (Unit 1 and Unit 3). The overall height of the aggregate is 11.2 meters, with dimensions of 24 meters in length and 12.6 meters in width. The external walls maintain a uniform thickness of 50 cm, whereas internal and shared walls have a 50 cm thickness at the base, transitioning to 30 cm thickness in the upper stories. The geometry of the building is reported in Figure 4. The slab is composed by wood beams to which all vertical loads with exception of the self-weight of masonry are applied. The modelling of the different slab typologies follows the premises explained in section 2.1 and was discretized using a mesh size of 30x30cm. Although numerical results remained consistent when tested with a mesh size up to 600 mm, a mesh size of 30x30 cm was chosen to establish a balance between the quality of the cracking plot and the analysis speed. Additionally, individual models of each unit were created to compare their behaviour as isolated structures and in aggregate configuration. Table 2 summarizes all the models created, which amounts to a total of eight models for each analysis.

All models were first analysed using non-linear static analysis using a lateral load profile proportional to the first mode of vibration to measure the response in terms of displacement at the top and reaction force at the base. Secondly, a component of the ground motion recorded from L'Aquila 2008 earthquake was introduced in the longitudinal direction of the aggregates and the recorded response was contrasted with the one obtained during monotonic analysis. Results were extracted from the longitudinal walls exclusively (Front, Middle and Back Walls) to avoid duplication of results extracted from shared transverse walls.

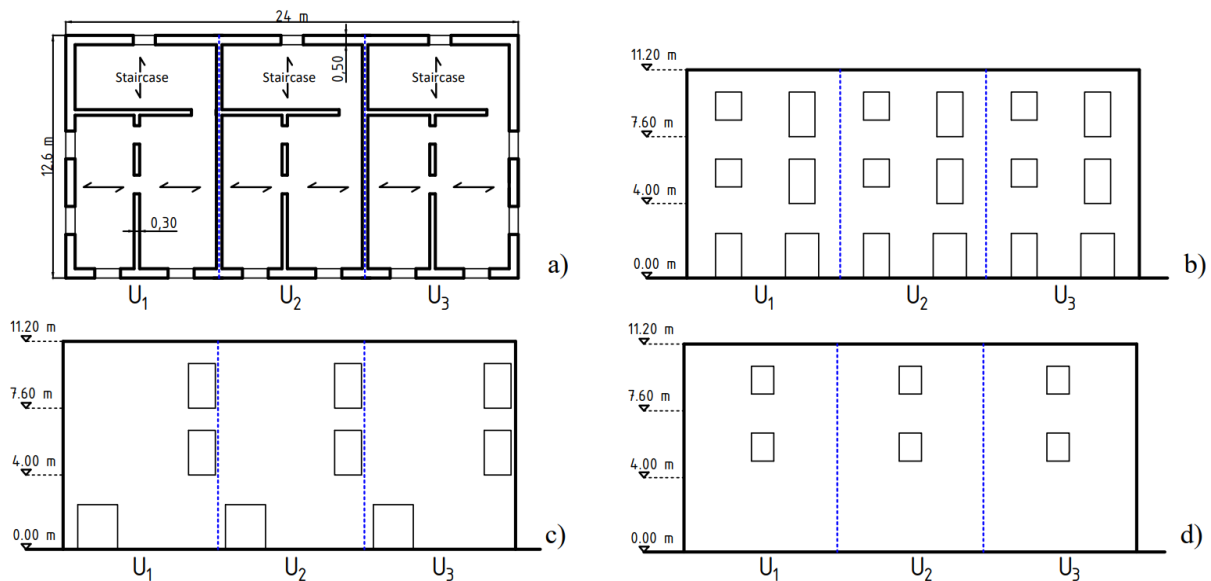


Figure 4. Aggregate geometry: a) plan view; b) Front Wall; c) Middle Wall; d) Back Wall.

Table 2. Cases of study.

| Diaphragm type | Unit configuration | Structure                  |
|----------------|--------------------|----------------------------|
| Rigid          | In aggregate       | Aggregate                  |
|                | Isolated           | Unit 1<br>Unit 2<br>Unit 3 |
| Flexible       | In aggregate       | Aggregate                  |
|                | Isolated           | Unit 1<br>Unit 2<br>Unit 3 |

### 3 Numerical response of aggregate buildings

#### 3.1 Rigid Diaphragm

The modal analysis used to calculate the lateral force profile exhibited a box-like behavior, with the first two modes being translational in the longitudinal and transverse directions, and a third mode representing rotational movement about the vertical axis. Results from the monotonic analysis, exhibited in Figure 5, showed an increase in resistance of the units (duplicating it in some cases) when considered within the aggregate configuration. The shape of the curve was characterized by a significant peak, followed by a softening phase. However, the resistance increment was influenced by the unit's position within the formation and the direction of the lateral force. For instance, Unit 1 experienced the increment when the aggregate was pushed in the negative direction, while it was absent when pushed in the positive direction. The opposite effect was observed in Unit 3. Unit 2 exhibited similar behaviour in both directions. In general, the findings showed that the aggregate configuration had a notable positive impact, which varied depending on the placement of individual units and the load direction.

When comparing these results with the dynamic response, it was evident that the former aligns well with the pushover curves in terms of stiffness during the elastic phase. However, this input was unable to push the structure into the softening phase. Therefore, it is currently inconclusive whether the pushover analysis can accurately capture the dynamic behaviour. On the other hand, it was observed that isolated units suffered a higher displacement demand when subjected to the same input when considered as isolated structures. Consequently, it was possible to observe the beginning of the softening phase in alignment with the monotonic curves, although this aspect should be further investigated.

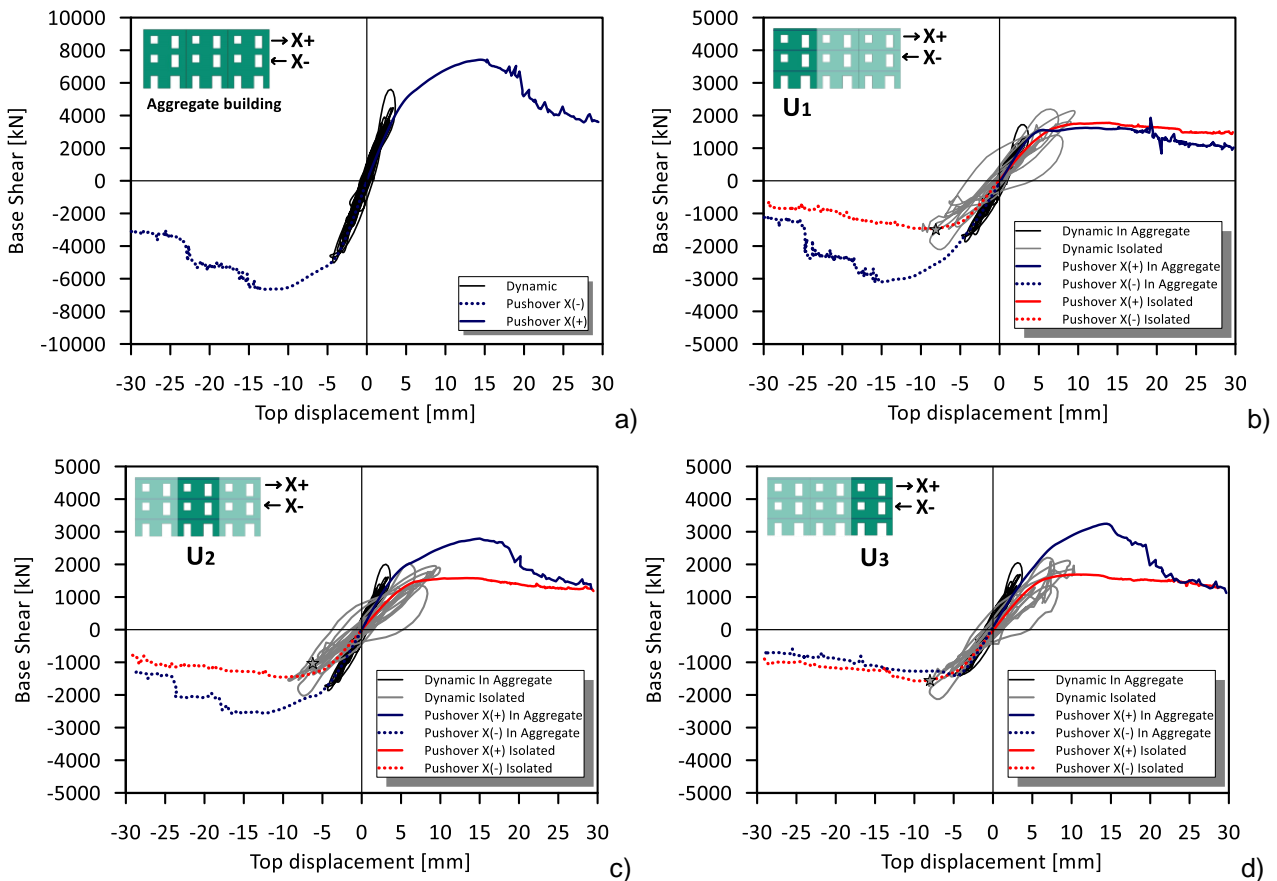


Figure 5. Results comparison between monotonic and dynamic analysis of the Rigid Diaphragm case: a) Aggregate building; b) Unit 1; c) Unit 2; d) Unit 3.

#### 3.2 Flexible Diaphragm

The analysis procedure used for the rigid diaphragm scenario was also employed to assess the flexible diaphragm case study. Modal analysis highlighted the differences in the dynamic behaviour related to the

flexibility of the slab. Local modes played a more significant role, and the distribution of loads on the walls corresponded to the mass they were supporting. This distribution was discernible through the difference in observed displacement for each wall. Pushover curves (Figure 6), instead, illustrated that the aggregate building behaves quite similarly to the previous case. However, with the activation of the aggregate effect, it does not deliver the same level of increment in resistance (maximum resistance of the aggregate of 5000 kN) and the curve lacks a distinct peak, as observed earlier. Nonetheless, the aggregate effect remained beneficial overall.

In the dynamic results, cycles were observed in alignment with the elastic phase of the monotonic response. Notably, the flexible diaphragm case imposed higher displacement demands compared to the rigid diaphragm, resulting in more accumulated damage and eventual collapse, even in aggregate configuration.

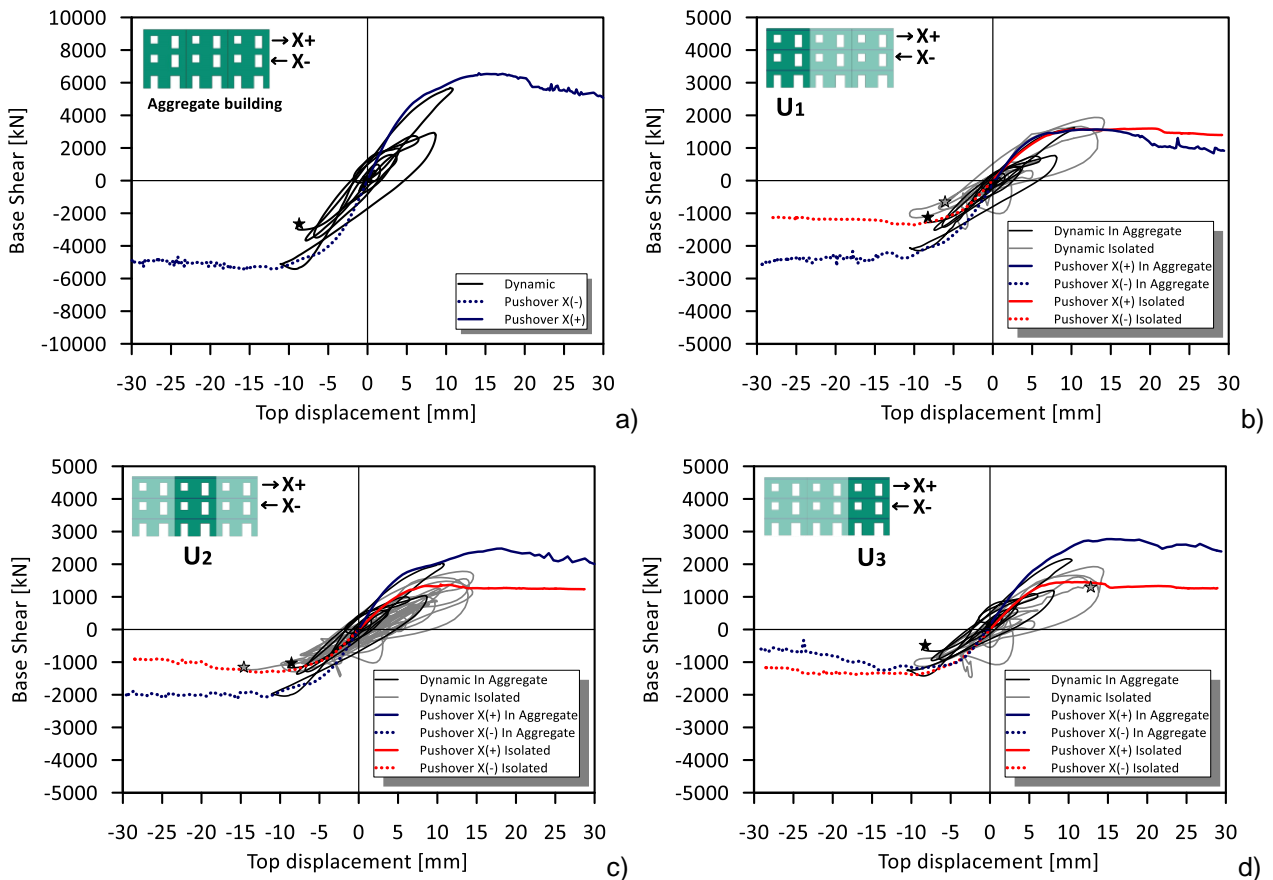


Figure 6. Results comparison between monotonic and dynamic analysis of the Flexible Diaphragm case: a) Aggregate building; b) Unit 1; c) Unit 2; d) Unit 3.

The maximum principal force plots that evidence the crack pattern of both rigid and flexible slabs are compared in Figure 7. The images emphasize the differences in wall displacement resulting from the presence of the flexible slab. The most prominent illustration of this effect is the exacerbated damage of the base piers of the front wall, in Figure 7.c, triggered by the significant displacement of the Front Wall. This is primarily due to the Front Wall being more flexible in combination with a stiffer Back Wall. The dynamic analysis results are compared in Figure 8, where it is possible to observe that the Rigid Diaphragm case presents reduced damage, mostly concentrated in the spandrels, while the Flexible Diaphragm damage pattern closely aligns with the results obtained in the pushover. The dynamic analysis results further confirm the flexible case's inclination to induce out-of-plane mechanisms in the transverse walls.



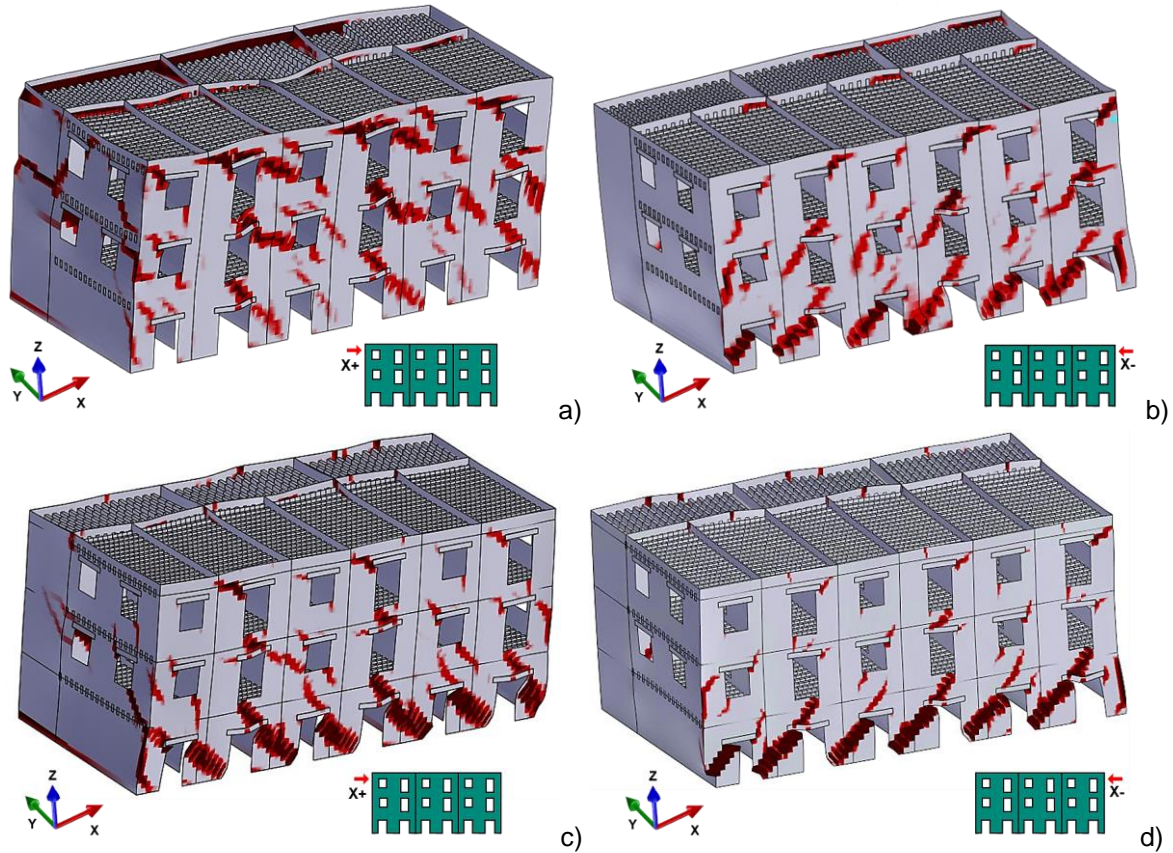


Figure 7. Crack pattern from monotonic analysis: a) Rigid Diaphragm X(+); b) Rigid Diaphragm X(-); c) Flexible Diaphragm X(+); d) Flexible Diaphragm X(-)

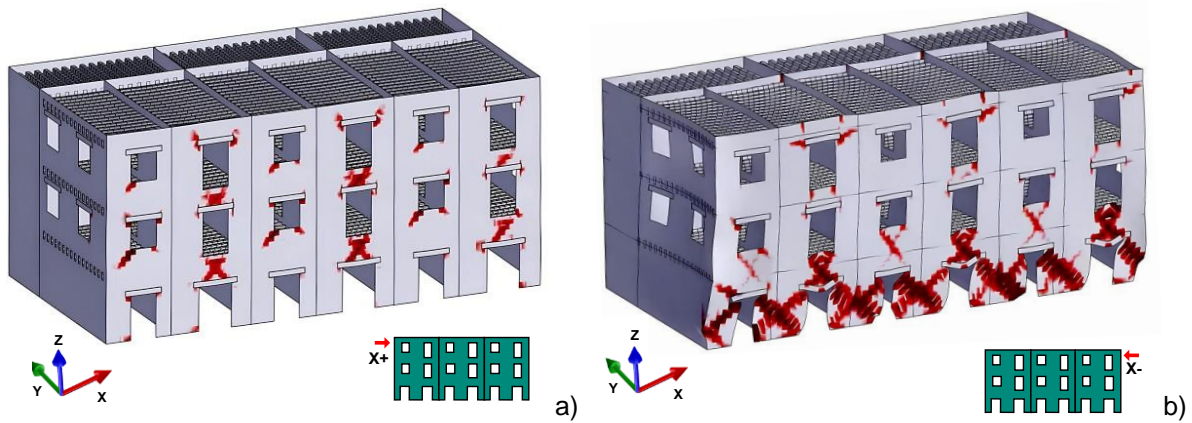


Figure 8. Crack pattern on walls from dynamic analysis: a) Rigid Diaphragm, b) Flexible Diaphragm

#### 4 Conclusions

The seismic behavior of building aggregates is intricate due to the diverse configurations and varying degrees of structural unit connections. Analyzing and assessing these systems in common practice involves numerous modeling uncertainties. Within this context, our study delved into the response of a three-unit unreinforced masonry aggregate to explore the potential benefits of what's known as the "aggregate effect".

Using STKO, a software platform for OpenSees, the aggregate effect was investigated in a reference building consisting of three similar units applying the homogenized masonry approach as a modelling strategy. Analysis included modal analysis, non-linear static analyses in both longitudinal directions, and a non-linear dynamic analysis. The responses of individual units within the aggregate and as isolated structures were recorded and compared, considering scenarios with both rigid and flexible slabs and assuming a rigid unit-to-unit connection.

The study revealed that the aggregate effect increases the resistance of the individual units, but its activation is conditioned by the unit's position within the aggregate. Moreover, the magnitude of this increment was shown to be dependent on the slab type, being rigid the most favorable case. Secondly, while pushover curves closely matched dynamic analysis during the elastic phase, it's important to note that the aggregate dynamic curve does not reach the softening phase. Thus, the pushover analysis's ability to capture dynamic behavior remains unclear and should be further investigated.

## 5 Acknowledgments

This study was carried out within the RETURN Extended Partnership and received funding from the European Union Next-GenerationEU (National Recovery and Resilience Plan – NRRP, Mission 4, Component 2, Investment 1.3 – D.D. 1243 2/8/2022, PE0000005)

## 6 References

- Angiolilli, M., Lagomarsino, S., Cattari, S. & Degli Abbatì, S. (2021). Seismic fragility assessment of existing masonry buildings in aggregate. *Engineering Structures*, 247: 0141-0296.
- Angiolilli, M., Pinasco, S., Cattari, S. & Lagomarsino, S. (2023). On the vulnerability features of historical masonry buildings in aggregate. *Procedia Structural Integrity*, 44: 2074-2081.
- fib special activity group, Taerwe, L., & Matthys, S. (2013). *fib model code for concrete structures 2010*
- Anthoine, A., Maganotte, G. & Magenes, G. (1995). Shear-compression testing and analysis of brick masonry walls. *Proceedings of the 10th European conference on earthquake engineering*, 3:
- Bernardini, C. et al., 2019. The seismic performance-based assessment of a masonry building enclosed in aggregate in Faro (Portugal) by means of a new target structural unit approach. *Engineering Structures*, 191: 386–400.
- Binda, L., Roberti, G. M. & Abbaneo, C. T. e. S. (1994). Measuring masonry material Properties. *Proceeding of the U.S.-Italy Workshop on Guidelines for Seismic Evaluation and Rehabilitation of Unreinforced Masonry Buildings (Technical report NCEER-94-0021)*, 6: 3-24.
- Brunelli, A., de Silva, F. & Cattari, S. (2022). Observed and simulated urban-scale seismic damage of masonry buildings in aggregate on soft soil: The case of Visso hit by the 2016/2017 Central Italy earthquake. *International Journal of Disaster Risk Reduction*, 83: 2212-4209.
- Chen, X.-M., Cen, S., Long, Y.-Q. & Yao, Z. H. (2004). Membrane elements insensitive to distortion using the quadrilateral area coordinate method. *Computers and Structures*, 82: 35-54.
- Ferrito, T., Milosevic, J. & Bento, R. (2016). Seismic vulnerability assessment of a mixed masonry-C building aggregate by linear and nonlinear analyses. *Bulleting of Earthquake Engineering*, 14: 2299-2327.
- Magenes, G. & Calvi, G. (1994). Experimental Research on Response of URM Building Systems. *Proceeding of the U.S.-Italy Workshop on Guidelines for Seismic Evaluation and Rehabilitation of Unreinforced Masonry Buildings (Technical report NCEER-94-0021)*, 22-24 June.
- Magenes, Kingsley & Calvi, 1995. Seismic Testing of a Full-Scale, Two-Story Masonry Building: Test Procedure and Measured Experimental Response.
- McKenna, F., Fenves, G. & Scott, M. (2000). *Open system for earthquake engineering simulation*. University of California, Berkeley, CA.
- Olive, J., A. H. & Cante, J. (2008). An implicit/explicit integration scheme to increase computability of non-linear material and contact/friction problems. *Computer Methods in Applied Mechanics and Engineering*, 197: 1865-1889.
- Petracca, M., Camata, G., Spacone, E. & Pelà, L. (2023). Efficient Constitutive Model for Continuous Micro-Modeling of Masonry Structures. *International Journal of Architectural Heritage*, 134-146.
- Petracca, M., Candeloro, F. & Camata, G. (2017). *ASDEA Software STKO user manual*.
- Ulrich, T., Negulescu, C. & Ducellier, A. (2015). Using the discrete element method to assess the seismic vulnerability of aggregated masonry buildings.. *Bulletin of Earthquake Engineering*, 13: 3135-3150.

- Valente, M., Milani, G., Grande, E. & Formisano, A. (2019). Historical masonry building aggregates: advanced numerical insight for an effective seismic assessment on two-row housing compounds. *Engineering Structures*, 190: 360-379.
- Xie, L. et al. (2015). A multi-layer shell element for shear walls based on OpenSEES. *Finite Elements in Analysis & Design*, 98: 14-25.